UNIVERSITY OF CALIFORNIA
IRVINE

CENTER FOR PERVASIVE COMMUNICATIONS AND COMPUTING

GRADUATE FELLOWSHIP PROJECTS PROGRESS REPORTS WINTER 2008

PROJECTS

ALPHABETIZED ACCORDING TO STUDENT LASTNAME

STUDENT NAME	PROJECT TITLE	ADVISOR
LUAY AZZAM	DECODING COMPLEXITY OF QUASI-ORTHOGONAL SPACE-TIME CODES	ENDER AYANOGLU
ALIREZA S. BEHBAHANI	OPTIMIZING MIMO RELAY NETWORKS	AHMED ELTAWIL
VIVEK CADAMBE	OPTIMAL INTERFERENCE ALIGNMENT FOR WIRELESS NETWORKS	SYED A. JAFAR
FATEMEH FAZEL	PRACTICAL CODE DESIGN FOR RECONFIGURABLE MIMO SYSTEMS	HAMID JAFARKHANI
MINAS GJOKA	NOVEL USES AND MISUSES OF PEER-TO-PEER SYSTEMS	ATHINA MARKOPOULOU
AMIN JAHANIAN	AN ULTRAHIGH-SPEED ANALOG-TO-DIGITAL CONVERTER (ADC) IN 130NM CMOS	PAYAM HEYDARI
MAHYAR KARGAR	ADAPTIVE EQUALIZATION OF MULTIMODE FIBER CHANNELS IN 0.13µM CMOS	MICHAEL GREEN
AMIN KHAJEH DJAHROMI	CHALLENGES AND OPPORTUNITIES IN DESIGNING ULTRA EFFICIENT COMMUNICATION SYSTEMS IN HIGHLY SCALED TECHNOLOGIES	AHMED ELTAWIL
SEUNG EUN LEE	POWER-AWARE INTERCONNECTION NETWORK FOR WIRELESS MOBILE SYSTEMS	NADER BAGHERZADEH
MOHAMMAD A. MAKHZAN	FAULT TOLERANT VOLTAGE SCALABLE CACHES	FADI KURDAHI
NEGAR NEJATI	OPTIMAL TRANSMISSION OF PACKETIZED VIDEO OVER TANDEM CHANNEL	HAMID JAFARKHANI
HULYA SEFEROGLU	NETWORK CODING FOR PRACTICAL APPLICATIONS OVER WIRELESS MESH NETWORKS	ATHINA MARKOPOULOU
VOLKAN SEVINDIK	USE OF BEAMFORMING IN ORTHOGONAL FREQUENCY DIVISION MULTIPLEXING	ENDER AYANOGLU
SRINIVASAN SURENDRAN	CAN INTERFERENCE ALIGNMENT DOUBLE THE CAPACITY OF AN INTERFERENCE NETWORK WITH CHANNEL UNCERTAINTY AND LIMITED POWER?	SYED A. JAFAR

Progress Report on Sphere Decoding Research: Winter 2008

Luay Azzam, Advisor: Ender Ayanoglu
Center for Pervasive Communications and Computing
Department of Electrical Engineering and Computer Science
The Henry Samueli School of Engineering
University of California, Irvine

***Abstract*— We propose a proper tree search traversal technique that reduces the overall sphere decoding computational complexity without sacrificing the performance. We exploit the similarity among the complex symbols in a square QAM lattice representation and rewrite the squared norm ML metric in a simpler form allowing significant reduction of the number of operations required to decode the transmitted symbols. We also show that this approach achieves $> 45\%$ complexity gain for systems employing 4-QAM, and that this gain becomes bigger as the constellation size is larger.**

I. Introduction

Different techniques have been proposed in the literature to reduce the complexity of SD. Among these, the increased radius search (IRS) [1] and the improved increasing radius search (IIRS) [2] are noteworthy. These two techniques attempt tackling this complexity by making a proper choice of the sphere radius. Other methods such as the application of the K-best lattice decoder [3] or a combination of the SD and the K-best decoder [4] were used where the complexity reduction came at the cost of a BER performance degradation.

In Winter 2008, we focused on reducing SD computational complexity. We improved the SD complexity efficiency by reducing the number of computations required to obtain the ML optimal solution. This complexity reduction was accomplished by exploiting the similarity between the complex symbols in a square QAM lattice representation. The proposed technique is generic and can be used with depth-first and breadth-first sphere decoders. Moreover, we showed that the conventional ML metric can be rewritten in a simpler form which can be also used for reduced complexity ML decoding. In our previous work presented in [5], we proposed a new lattice representation that enables decoding the real and imaginary parts of each complex symbol independently. In this work, we used that same lattice representation and showed that a complexity gain of at least 45% can be obtained without sacrificing the performance.

II. Computational Complexity

We have considered 2×2, 4×4 systems using 4-QAM, 16-QAM and 64-QAM modulation schemes. Since the multiplications are the most expensive operations in terms of machine cycles compared to additions, the complexity is measured in terms of the number of real multiplications required to decode the transmitted complex symbols. We use the real-valued lattice representation presented in [5] for the conventional and proposed SD. This means that the complexity gain shown in all the figures below is on top of the gain obtained in [5]. We denote the conventional SD by Conv and the proposed SD by PR.

Figure 1 shows the complexity curves for both algorithms using 4-QAM. For 2×2 system, the complexity gain is 45%. This gain increases up to reach 60% for the 4×4 case.

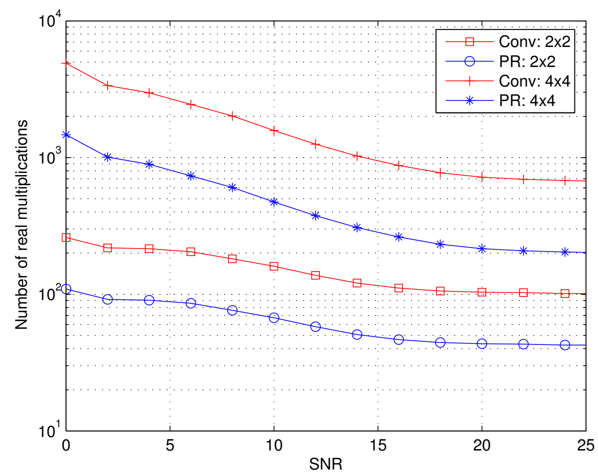

Fig. 1. Number of real multiplications vs SNR for the proposed and conventional SD over a 2×2, and 4×4 MIMO flat fading channel using 4-QAM.

References

[1] E. Viterbo and J. Boutros, “A Universal Lattice Code Decoder for Fading Channels,” *IEEE Trans. Inform. Theory*, vol. 45, no. 5, pp. 1639–1642, Jul. 1999.

[2] W. Zhao and G. Giannakis, “Sphere Decoding Algorithms With Improved Radius Search,” *IEEE Trans. Commun.*, vol. 53, pp. 1104–1109, Jul. 2005.

[3] K. Wong, C. Tsui, R.-K. Cheng, and W. Mow, “A VLSI architecture of a K-best lattice decoding algorithm for MIMO channels,” *in Proc. IEEE ISCAS02*, vol. 3, pp. 273–276, 2002.

[4] J. Tang, A. Tewfik, and K.K.Parhi, “Reduced Complexity Sphere Decoding and Application to interfering IEEE 802.15.3a piconets,” *IEEE ICC*, vol. 5, pp. 2864–2868, June 2004.

[5] L. Azzam and E. Ayanoglu, “Reduced Complexity Sphere Decoding for Square QAM via a New Lattice Representation,” *IEEE GLOBECOM*, pp. 4242–4246, Nov. 2007.

Progress Report on "Relay Networks"
Winter 2008

Alireza S. Behbahani, Advisor: Prof. Ahmed Eltawil
Electrical Engineering Department
University of California, Irvine, USA
Email: sshahanb@uci.edu

In Winter 2008 quarter, we started working on channel estimation for SISO relay networks. We design and analyze a training based linear mean square error (LMMSE) channel estimator for time division multiplex amplify-and-forward (AF) relay networks. We started with the scenario where relays have no knowledge of their backward and forward channels.

We consider an AF relay network consisting of 1 transmit antenna at the source, 1 receive antenna at the destination, and K relays, each equipped with 1 antenna. We denote by h_{s_i} the channel between the source and relay i, backward channel, while h_{t_i} is the channel between the relay i and the destination, forward channel. We assume that the channels follow the block-fading law, where the channels are constant for some coherence interval T_c, which is measured in symbols, and after that they change to an independent value which hold for another interval T_c. We further assume that channel estimation and data transmission is to be done during the interval T_c. Also backward and forward channels are independent and Rayleigh flat fading distributed which are $h_{s_i},\ h_{t_i} \sim \mathcal{CN}(0, \sigma_h^2), \quad i = 1, \cdots, K$ and where for convenience we assumed that backward and forward channels have the same variance, σ_h^2.

In the first phase transmitter sends the signal block $\boldsymbol{s} = [s_1, \cdots, s_{T_c}]^T$ to the relays. The received signal at relay i can be modeled as

$$\boldsymbol{r}_i = h_{s_i}\boldsymbol{s} + \boldsymbol{v}_{s_i}, \tag{1}$$

where $\boldsymbol{r}_i = [r_{i_1}, \cdots, r_{i_{T_c}}]^T$ is the received signal and $\boldsymbol{v}_{s_i} = [v_{s_{i_1}}, \cdots, v_{s_{i_{T_c}}}]^T$ is the zero mean additive white complex Gaussian noise at the relay i with covariance matrix $\boldsymbol{R}_{\boldsymbol{v}_{s_i}} = \sigma_{v_s}^2\boldsymbol{I}$. Also the transmitter has the total power $\mathsf{E}\boldsymbol{s}^*\boldsymbol{s} = T_cP_s$, where P_s is the average transmitting power of the source. In the second phase each relay, multiplies its received signal by a scalar coefficient β_i which is constant during coherence time T_c and sends it, on the same time slot, to the destination. The received signal at the destination can be expressed as

$$\boldsymbol{y} = \sum_{i=1}^{K}\beta_i\boldsymbol{r}_i h_{t_i} + \boldsymbol{v}_t, \tag{2}$$

where $\boldsymbol{v}_t$ is $T_c \times 1$ zero mean additive white complex Gaussian noise at the destination with covariance matrix $\boldsymbol{R}_{\boldsymbol{v}_t} = \sigma_{v_t}^2\boldsymbol{I}$ and also independent of $\boldsymbol{v}_{s_i}$ for all i. By plugging (1) in (2) the received signal can be expressed as

$$\boldsymbol{y} = \underbrace{\sum_{i=1}^{K}\beta_i h_{s_i}h_{t_i}}_{h_{tot}}\boldsymbol{s} + \underbrace{\sum_{i=1}^{K}\beta_i h_{t_i}\boldsymbol{v}_{s_i} + \boldsymbol{v}_t}_{\boldsymbol{n}} = h_{tot}\ \boldsymbol{s} + \boldsymbol{n}, \tag{3}$$

where h_{tot} is the overall channel from the source to the destination and $\boldsymbol{n}$ is the overall noise at the destination which is zero mean and has the covariance matrix

$$\boldsymbol{R}_n = (\sigma_{v_s}^2\sigma_h^2\sum_{i=1}^{K}|\beta_i|^2 + \sigma_{v_t}^2)\boldsymbol{I} = \sigma_n^2\boldsymbol{I}\ . \tag{4}$$

Since the receiver does not know h_{tot}, training-based schemes assign part of the transmitted signal $\boldsymbol{s}$ to be a known training signal from which the receiver can learn h_{tot}.

Here, relays just scale and forward its received signal to the destination and they do not have any knowledge of the backward and forward channels. Here the transmission starts by sending training symbols from the transmitter to the destination through relays and there is no need for training symbols from the receiver and also estimation at each relay. The scaling factor is given by

$$\beta_i = \sqrt{\frac{P_r}{\sigma_h^2P_s + \sigma_{v_s}^2}}\ , \tag{5}$$

where P_r is the output power of each relay. The expression $\sqrt{\frac{P_r}{P_s+\sigma_{v_s}^2}}$ adjusts the output power of relays from long term point of view. Also conservation of time yields

$$T_c = T_\tau + T_d\ . \tag{6}$$

In order to investigate the performance of our proposed channel estimation We define the signal to noise ratio as SNR $= P_s/\sigma_{v_s}^2$, where $\sigma_{v_s}^2 = \sigma_{v_t}^2$ and also $\sigma_h^2 = 1$. We further assume that the transmitter output power, P_s, and the relays average output power, P_r, are set to 10 dB.

Figure 1 shows channel estimation mean square error (MSE) for the case that relays do not have knowledge of channels for coherence interval of $T_c = 300$ and training interval of $T_\tau = 10$. It can be seen that increasing the number of relays increases the MSE which is consistent with mathematical analysis where it says that estimation error variance increases with K.

We are going to continue this work by considering the total channel estimation between the source and destination for two other scenarios where, each relay knows its backward and forward channels perfectly, and each relay estimates its backward and forward channels. The scenario where each relay estimates its backward and forward channels is a general case for the other two scenarios. Finally, we find a lower bound for the capacity considering the effect of training and estimation error.

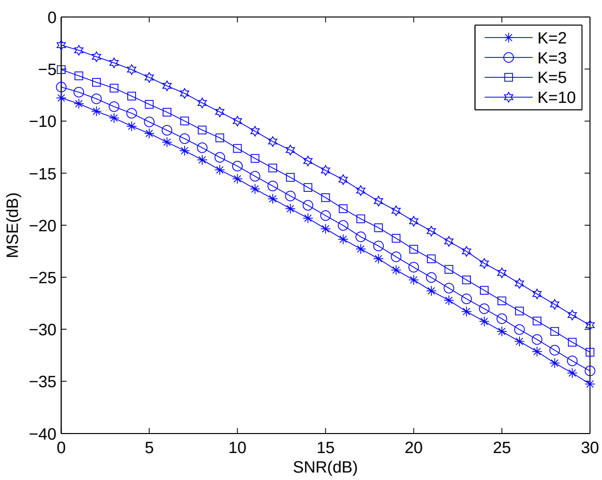

Fig. 1. MSE in dB versus SNR for $T_c = 300$, and $T_\tau = 10$ for different number of relays. Here relays do not have knowledge of their backward and forward channels.

Progress in Winter 2008 : The Impact of Relays, Feedback, Cooperation and Full-Duplex Operation on the Capacity of Wireless Networks

Viveck R. Cadambe, Syed A. Jafar
Center For Pervasive Communications and Computing Electrical Engineering and Computer Science
University of California Irvine,
Irvine, California, 92697, USA
Email: vcadambe@uci.edu, syed@uci.edu

***Abstract*— In this winter 2008 report, we study the capacity of fully connected wireless networks within $o(\log(\mathbf{SNR}))$ bits where SNR represents the signal to noise ratio. We first consider a network with S source nodes, R relay nodes and D destination nodes with full duplex operation allowed at all nodes. We also allow feedback to all source and relay nodes. The sum capacity of this network is characterized in this paper as $\frac{SD}{S+D-1}\log(\mathbf{SNR}) + o(\log(\mathbf{SNR}))$. The implication of the result is that relays, perfect feedback to source/destination nodes, noisy cooperation and full duplex operation can only improve the capacity of this network by a factor of $o(\log(\mathbf{SNR}))$.**

I. Introduction

Previous work in fall 2007 established, within $o(\log(\text{SNR})$, the capacity of $S \times D$ X network i.e. a network with S sources, D destinations and SD messages - one message for each source-destination pair. It was shown that the capacity of this network maybe characterized as

$$C(\text{SNR}) = \frac{SD}{S+D-1}\log(\text{SNR}) + o(\log(\text{SNR})) \quad (1)$$

Equivalently, the X network has $\frac{SD}{S+D-1}$ degrees of freedom. The coding scheme achieving the above rate was based on the idea of interference alignment ([1] and references therein). The model of the X network was a single-hop network with half-duplex transmit and destination nodes. The model precluded various known techniques used to improve the rates of communication in wireless networks such as relays, feedback, transmit/receive co-operation and full duplex operation. In this work, we extend the model of the X network to include these techniques and study the degrees of freedom of the resultant network. Specifically, we consider the fully connected $S \times R \times D$ wireless network i.e. a network with S full duplex source nodes, D full duplex destination nodes and R relays. There are SD independent messages in the network- one message between each source node and each destination node. We allow noisy co-operation between source nodes and destination nodes. Further, we also allow for perfect feedback from all destination nodes to all the source nodes. We also assume that the network is fully connected meaning that the channel gain between any two nodes is non-zero. Our main result presented in the next section is the degrees of freedom characterization of this network.

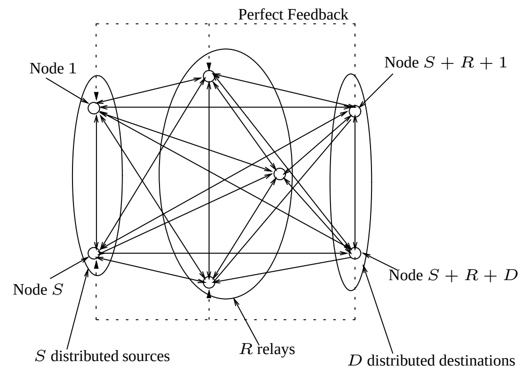

Fig. 1. The $S \times R \times D$ network

II. Summary of Results

The main result of this report is the following.

Theorem 1: The sum capacity $C(\text{SNR})$ of the fully connected $S \times R \times D$ wireless network may be expressed as

$$C(\text{SNR}) = \frac{SD}{S+D-1}\log(\text{SNR}) + o(\log \text{SNR})$$

Equivalently, the fully connected $S \times R \times D$ wireless network has $\frac{SD}{S+D-1}$ degrees of freedom.
Note that the capacity characterization within $o(\log(\text{SNR}))$ of the fully connected $S \times R \times D$

network above is identical to that of the $S \times D$ X network in equation (1). Since the $S \times R \times D$ network is a generalization of the X network, the interference alignment based achievable scheme for the X network presented in [2] simply extends to the $S \times R \times D$ network. The converse argument (i.e. outerbound) is however, not a trivial extension of the converse for the X network. The proof of the converse is presented in the full paper [3]. The theorem implies that, quite surprisingly, the techniques of relays, feedback, co-operation and full duplex operation cannot improve the degrees of freedom of a fully connected wireless network. They can only provide capacity improvements upto a $o(\log(\text{SNR}))$ term. The search for improvements of the order of $\log(\text{SNR})$ in wireless networks ends in interference alignment. There are, however, a few exceptions precluded by our system model where these techniques can improve the degrees of freedom. We only list these exceptions below - the reader is referred to [3] for the details.

1) Relays can improve the degrees of freedom if a network is not fully connected.
2) Co-operation can increase the degrees of freedom if the cost of co-operation is not accounted for (i.e. in genie aided networks)
3) Full duplex operation can increase the degrees of freedom if source nodes can also be destination nodes
4) Feedback can improve the degrees of freedom if it is provided to a destination node

REFERENCES

[1] S. A. Jafar and S. Shamai, “Degrees of freedom region of the mimo x channel,” *Information Theory, IEEE Transactions on*, vol. 54, no. 1, pp. 151–170, Jan. 2008.

[2] V. R. Cadambe and S. A. Jafar, “Degrees of freedom of wireless x networks,” *arxiv.org*, 2007. arxiv eprint = cs/0711.2824.

[3] V. R. Cadambe and S. A. Jafar, “Capacity of wireless networks within o(log(snr)) - the impact of relays, feedback, co-operation and full-duplex operation,” *arxiv.org*, Feb 2008. eprint - arxiv:0802.0534.

State-Selection in a Space-Time-State Block Coded MIMO Communication System

Fatemeh Fazel, Advisor: Hamid Jafarkhani
Center for Pervasive Communications and Computing
EECS, University of California, Irvine
{fazel,hamidj}@uci.edu

I. Project Motivation

In [1], we proposed a state-switching scheme for reconfigurable MIMO systems, when the transmit antenna is reconfigurable. In this work we study the case when the receiver antenna is reconfigurable. We propose state-selection in combination with Space-Time-State (STS) block coding and prove that the aforementioned scheme is capable of achieving maximum diversity gains as well as additional selection gains compared to state-switching.

II. Progress Report

For perfect channel estimation, the instantaneous post-processed SNR at the receiver of a reconfigurable MIMO system using STS codes of duration Ψ is given by,

$$SNR = \frac{||\mathbf{H}_1||^4 + \cdots + ||\mathbf{H}_\Psi||^4}{2\sigma_n^2(||\mathbf{H}_1||^2 + \cdots + ||\mathbf{H}_\Psi||^2)} \quad (1)$$

where, $||\mathbf{H}_\psi||^2 = |h_1^\psi|^2 + |h_2^\psi|^2$ for state $\psi \in \{1, \ldots, \Psi\}$.

A. Optimal Selection Algorithm

The optimal selection criterion is to choose the P states, $\{i_1, \ldots, i_P\}$ such that,

$$\arg max_{\substack{i_1,\ldots,i_P \\ 1\le i_1,\ldots,i_P \le P}} \frac{||\mathbf{H}_{i_1}||^4 + \cdots + ||\mathbf{H}_{i_P}||^4}{||\mathbf{H}_{i_1}||^2 + \cdots + ||\mathbf{H}_{i_P}||^2} \quad (2)$$

B. An Ad hoc Selection Algorithm

We propose an ad hoc selection criterion with a simple format and prove that it achieves maximum diversity gains. Later, we prove that in fact the ad hoc selection algorithm is equivalent to the optimal selection algorithm. The ad hoc selection scheme chooses P channel propagation states, $\{\mathbf{H}_{i_1}, \ldots, \mathbf{H}_{i_P}\}$ out of the total of Ψ available states, such that:

$$\{i_1, \ldots, i_P\} = \arg max_{\substack{i_1,\ldots,i_P \\ 1\le i_1,\ldots,i_P \le \Psi}} ||\mathbf{H}_{i_1}||^2 + \cdots + ||\mathbf{H}_{i_P}||^2 \quad (3)$$

Theorem 1: The ad hoc state-selection method given by (3), in combination with an STS-P code, achieves full-diversity of $M_T M_R \Psi$.

Proof: Let us make the simplifying assumption that $\mathbf{H}_i$'s are independent. The conditional pairwise error probability can be written as,

$$P(\mathbf{C}^1 \to \mathbf{C}^2|\mathbf{H}) = Q\left(\sqrt{\frac{\gamma}{2}\sum_{p=1}^{P} ||(\mathbf{C}_p^2 - \mathbf{C}_p^1)\mathbf{H}_p||_F^2}\right)$$

Note that using the STS code structure,

$$||(\mathbf{C}_p^2 - \mathbf{C}_p^1)\mathbf{H}_p||_F^2 = x_p \sum_{n=1}^{N}\sum_{m=1}^{M} |h_{n,m}^p|^2, \quad (4)$$

where, $x_p = |\mathcal{D}_{2p-1}|^2 + |\mathcal{D}_{2p}|^2$ and $\mathcal{D}_i = \mathcal{S}_i^2 - \mathcal{S}_i^1$ for all $i \in \{1, \ldots, 2P\}$. Let $x_{min} = \min\{x_1, \ldots, x_P\}$. Then,

$$\begin{aligned} \frac{P}{\Psi} x_{min} \sum_{p=1}^{\Psi} ||\mathbf{H}_p||_F^2 \le & \quad x_{min}\{||\mathbf{H}_1||_F^2 + \cdots + ||\mathbf{H}_P||_F^2\} \\ \le & \quad x_1||\mathbf{H}_1||_F^2 + \cdots + x_P||\mathbf{H}_P||_F^2 \end{aligned} \quad (5)$$

which results in,

$$P(\mathbf{C}^1 \to \mathbf{C}^2|\mathbf{H}) \le Q\left(\sqrt{\frac{\gamma}{2}\frac{P}{\Psi} x_{min} \sum_{\psi=1}^{\Psi} ||\mathbf{H}_\psi||_F^2}\right) \quad (6)$$

Now, using the chernoff upper bound and calculating the expected value with respect to h_{ij}^ψ's results in,

$$P(\mathbf{C}^1 \to \mathbf{C}^2) \le \left(\frac{1}{1 + \frac{\gamma P}{2\Psi}}\right)^{\Psi M_T M_R}. \quad (7)$$

■

Therefore, by using an ad hoc state-selection scheme one can achieve a diversity of $\Psi M_T M_R$, which is the highest level of diversity offered by the system.

C. Single-state Selection

In this subsection, we show that the optimal and the ad hoc criteria are equivalent and that they are equivalent to selecting the single best state.

Theorem 2: The optimal selection criterion, based on maximizing the received SNR, is equivalent to selecting the single best channel propagation state.

Proof: It is easy to show that, $\forall a_i \in \mathbb{R}$, where $i \in \{1,\ldots,m\}$,

$$z = \frac{a_1^4 + \cdots + a_m^4}{a_1^2 + \cdots + a_m^2} \leq \max_i a_i^2 \tag{8}$$

Using (8), one can show that

$$\max_{\substack{i_1,\ldots,i_P \\ 1\leq i_1,\ldots,i_P \leq P}} \frac{||\mathbf{H}_{i_1}||^4 + \cdots + ||\mathbf{H}_{i_P}||^4}{||\mathbf{H}_{i_1}||^2 + \cdots + ||\mathbf{H}_{i_P}||^2} = ||\mathbf{H}_{max}||^2 \tag{9}$$

where, $||\mathbf{H}_{max}||^2 = \max_{j\in\{1,\ldots,\Psi\}} ||\mathbf{H}_j||^2$. Therefore, the optimal selection algorithm chooses the best channel state and fixes the channel for the period of P codewords. ■

Also, the ad hoc selection criterion results in,

$$\max_{\substack{i_1,\ldots,i_P \\ 1\leq i_1,\ldots,i_P \leq P}} ||\mathbf{H}_{i_1}||^2 + \cdots + ||\mathbf{H}_{i_P}||^2 =$$
$$\max_{i_1} ||\mathbf{H}_{i_1}||^2 + \cdots + \max_{i_P} ||\mathbf{H}_{i_P}||^2 = P||\mathbf{H}_{max}||^2 \tag{10}$$

Therefore, both the optimal and ad hoc selection schemes resort to selecting the single best state, $\mathbf{H}_{max}$, and fixing the channel in that state, over the duration of P codeword transmissions.

D. Simulation Results

Figure 1 shows the BER-SNR performance of an ideally uncorrelated reconfigurable multi antenna system, with $\Psi = 5$ and $\Psi = 2$ for 1 bit/sec/Hz. We compare various state-switching and state-selection schemes and we characterize their performance according to three factors: diversity gain, coding gain and selection gain. As shown in this figure, for both state-switching and state-selection schemes, as the number of CPSs (Ψ) increases, a larger diversity order is achieved. For a fixed Ψ, by using an STS with a larger period (P), we obtain improvements through coding gain. Note, however, that using an STS with larger period results in higher decoding complexity and decoding delays. Both state-switching and state-selection schemes achieve full diversity therefore the slope of the BER curves in asymptotical high-SNR scenarios should eventually be the same. At the same diversity level, as one confers from the simulation results, at the low SNR region coding gain is a more dominant factor, while in high SNR region, selection gain becomes more dominant.

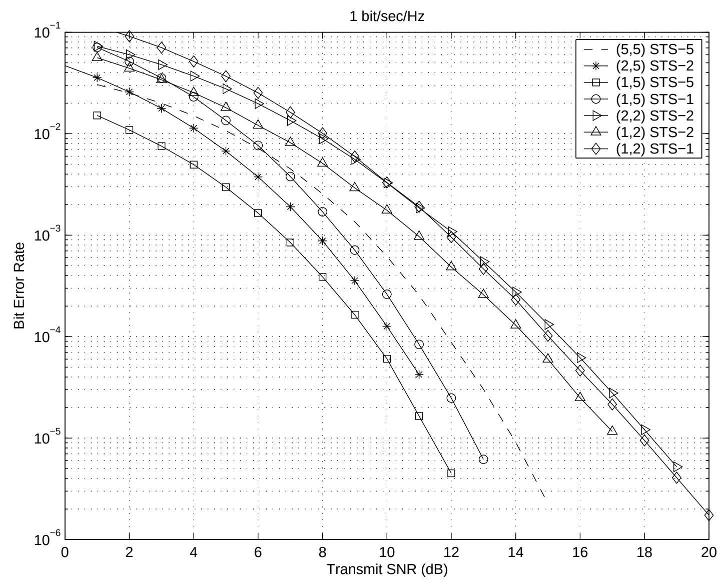

Fig. 1. BER vs. transmit SNR for an ideal reconfigurable multi-antenna system; 1 bit/sec/Hz using BPSK.

REFERENCES

[1] F. Fazel, A. Grau, H. Jafarkhani and F. De Flaviis, ”Space-Time Block Coded Reconfigurable MIMO Communication System Using ORIOL Antennas”, *Wireless Communication & Networking Conference* (WCNC) 2008.

Progress Report - Winter 2008

Minas Gjoka
Advisor: Athina Markopoulou
Center of Pervasive Communications and Computing
The Henry Samueli School of Engineering
University of California, Irvine
mgjoka@uci.edu

This quarter I was involved in two projects. In the first project, we characterize the popularity and user reach of Facebook applications. We analyze application usage data gathered over a period of six months. We also crawled publicly accessible Facebook user profiles to obtain per user application installation statistics. The paper [1] will appear in SIGCOMM Workshop on Online Social Networks (WOSN) 2008. In the second project [2], we propose a new practical IP traceback scheme which combines probabilistic packet marking with network coding.

I. Characterization of OSN Applications

A. Introduction

In a successful attempt to enhance user experience and increase the site's appeal, in May 2007, Facebook made a key innovation: they opened their platform to third-party developers. Developers are now able to create Facebook applications that augment Facebooks functionality or act as front-end to third party web-based services. In mid-February 2008, there were approximately 866M installations of 16.7K distinct Facebook applications, and 200K developers were utilizing the platform. As of today, more than 100 OSN application development companies have been founded and Facebook application based advertising campaigns have been surprisingly successful.

Motivated by this unprecedented success, we became interested in studying the popularity (both its distribution and change over time), and adoption dynamics (how applications are installed by users) of Facebook applications. An in-depth understanding of these characteristics is important both for engineering and marketing reasons. Understanding the popularity and adoption dynamics can assist advertisers and investors to form strategies for acquiring applications or purchasing advertising real-estate, so as to reach a large portion of the targeted user-base at a low cost. At the same time, determining which applications tend to attract more users, can help to better engineer the applications user interface and features and to better provision the OSN system.

B. Progress

We collected and analyzed two data sets pertaining to Facebook applications. The first data set provides the number of installations for each application and the number of distinct users that engage each application at least once during a day, for a period of 6 months. The second data set consists of a sample of publicly available Facebook user proles, crawled for 1 week in Feb. 2008, pertaining to approximately 300K users and 13.6K applications.

Our work makes the following contributions. We present the first study to characterize the statistical properties of OSN applications. Previous work focused on the characteristics of the social graph itself or the popularity of user generated content. In addition, we propose a simple and intuitive method to simulate the process with which users install applications. Using this method one can determine the user coverage from the popularity of applications, without detailed knowledge of how applications are distributed among users. We validate our model by comparing user coverage statistics obtained by the model and the crawled data set.

II. A Network Coding Approach to IP Traceback

A. Introduction

Traceback schemes aim at identifying the source(s) of a sequence of network packets and the nodes these packets traversed. This is, in particular, useful for tracing the sources of a Distributed Denial-of-Service (DDoS) attack. We are interested in the family of Probabilistic Packet Marking (PPM) schemes for IP traceback. The main idea is to have intermediate nodes mark packets probabilistically with information about their identity and the victim uses the information on the marked packets to reconstruct the paths.

B. Progress

We build on the insight that probabilistic traceback is essentially a Coupon Collector's Problem. We combine PPM with the idea of random linear network coding in our proposed PPM+NC scheme and show that this approach advances algebraic traceback. We then take the bit constraints into account and propose the practical PPM+NC scheme. In addition, we extend the idea of adjusted marking probabilities to multipath scenarios and exploit this idea in the adjusted practical PPM+NC scheme. Simulation results show that our schemes reduce the average number of packets needed for reconstruction which becomes extremely important in DDoS attacks.

References

[1] Minas Gjoka, Michael Sirivianos, Athina Markopoulou, Xiaowei Yang, "Poking Facebook: Characterization of OSN Applications", *to appear in Proc. of ACM SIGCOMM Workshop on Online Social Networks '08*

[2] Pegah Sattari, Minas Gjoka, Athina Markopoulou, "A Network Coding Approach to IP Traceback", *in preparation for journal publication*

Progress Report on Multiple-Antenna Front-End Design Research: Winter 2008

Amin Jahanian Advisor: Payam Heydari
Nanoscale Communications Integrated Circuits Lab
Center for Pervasive Communications and Computing
Department of Electrical Engineering and Computer Science
The Henry Samueli School of Engineering
University of California, Irvine, CA 92697-2625
Email: jahanian@uci.edu

Abstract — **In the winter quarter, we worked on incorporation of non-orthogonal codes on the previously designed multiple-antenna receiver architecture. The use of non-orthogonal codes makes it possible for us to decrease the BW expansion inherent in the code-modulated path-sharing multiple antenna (CPMA) receiver architecture. The CPMA receiver is capable of accommodating multiple input multiple output (MIMO) including spatial multiplexing, spatial diversity, and beamforming. The use of a unique code-modulation scheme at the RF stages of the signal paths enables linear combination of all mutually orthogonal code-modulated received signals. The combined signal is then fed to a single RF/baseband/ADC chain, resulting in a significant reduction of power consumption and area, as well as mitigating the issue of LO routing/distribution. In the digital domain, all antenna signals are fully recovered.**

I. INTRODUCTION

Multi-antenna communications promises higher data rates using spatial multiplexing (SM), and increased range using spatial diversity (SD) and beamforming (BF). The use of multiple antennas in any MIMO RX may entail multiple RF chains, baseband blocks and ADCs [1], [2]. Consequently, there will be considerable increase in power consumption and chip area. In addition, having multiple receive chains results in a complicated LO routing and distribution task.

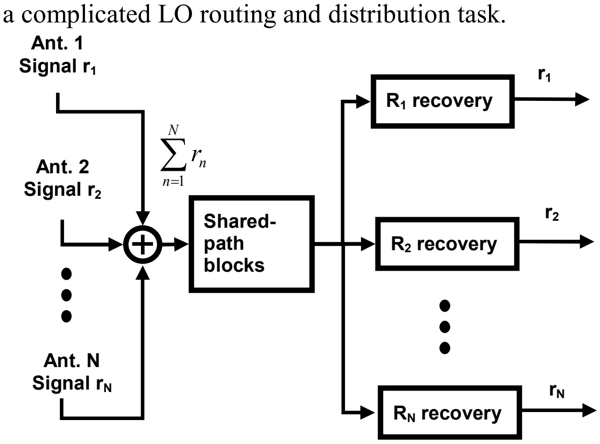

Fig. 1. Conceptual diagram of the proposed CPMA receiver

Previously in this project, we had presented a new **code-modulated path-sharing multi-antenna** (CPMA) RX front-end architecture (Fig. 2) that enables sharing of RF, baseband, and ADC blocks among multi-antenna signals. The underlying idea is to implement a code modulation system *within* the multi-antenna RX in order to distinguish antenna signals before combining them in the RF domain. More specifically, N antenna signals are modulated by N orthogonal code sequences. The mutual orthogonality of code-modulated signals allows signal combination in the RF domain, while promising full recovery of each signal in the baseband using digital matched filters (DMF). The recovered signal is then fed to the MIMO DSP for further processing. The proposed CPMA RX front-end is capable of accommodating any multi-antenna scheme, including SM, SD (including OSTBC, MRC, and BF). The advantages of this architecture include significant reduction of power consumption and chip area, and mitigation of coupling between antenna signals in the RX. Moreover, the single path alleviates the problem of LO distribution and routing in multi-antenna architectures.

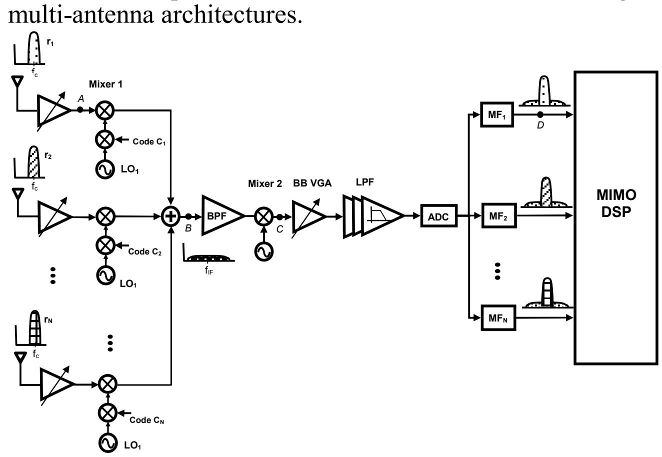

Fig. 2. Proposed CPMA receiver

II. EFFECT OF NON-ORTHOGONAL CODES ON CAPACITY

A. Effective Channel Matrix

To analyze the use of non-orthogonal codes, we derived the effective channel matrix representation that relates the outputs of the matched filters to **H**, **b**, **n**, and the cross-correlation between the codes. Each path in the receiver is multiplied by its designated code and then the resultant signals are summed, achieving a scalar quantity S. From here we can find at the outputs of the matched filters an $N\times1$ vector. From there, the effective channel matrix and effective noise matrix, $\mathbf{H}_{eff}$ and $\mathbf{n}_{eff}$, are found, respectively.

B. Effect on Capacity

We then investigated the impact of non-orthogonal codes on the MIMO capacity. Considering the effective channel and effective noise matrices, the capacity of the CPMA receiver was derived.

Fig. 3 plots the capacity as a function of ρ, and for various N's and a fixed E_s/N_0 of 30 dB. Observing this figure, the curves have a gradual negative slope for $\rho \leq 0.7$, while for $\rho > 0.7$ the curves drop sharply and the capacity is degraded severely. To get a better idea, for N=8, when ρ varies in 0.1 step sizes from 0 to 1, the capacity degrades by approximately 2%, 4%, 6%, 8%, 11 %, 13%, 17%, 22%, 31%, and 84%, respectively. This indicates that by keeping the code cross-correlation at appropriate values, we can achieve an acceptable tradeoff between capacity degradation and minimization of bandwidth requirements obtained by using non-orthogonal codes to accommodate $N>G$ antennas.

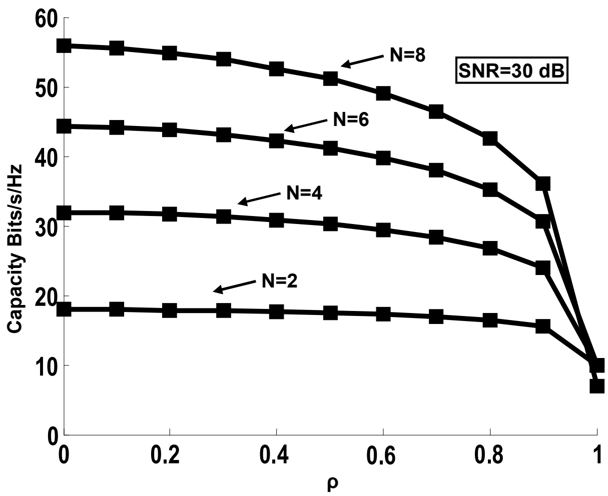

Fig. 3. Capacity vs. for various N.

Fig. 4 demonstrates the plot of capacity versus ρ for various SNR's for a 4×4 MIMO system. From these curves, it is evident that at high SNR's the capacity is affected by ρ more substantially, whereas at low SNR's the capacity is noise limited and is less affected by ρ.

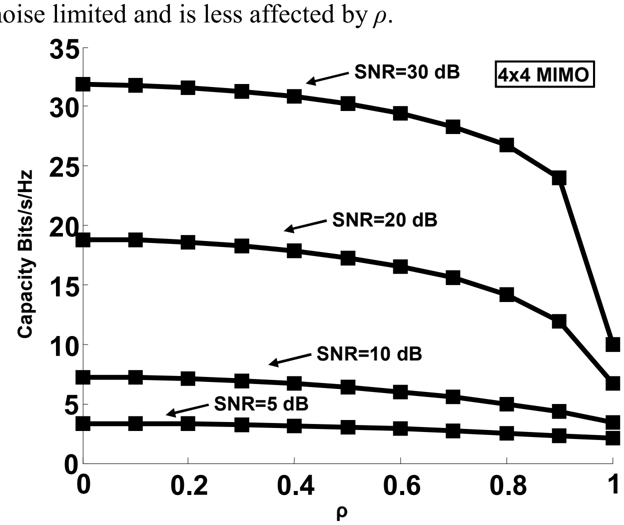

Fig. 4. Capacity vs. ρ for various SNRs.

REFERENCES

[1] A. Behzad, *et al*, "A fully integrated MIMO multi-band direct-conversion CMOS transceiver for WLAN applications (802.11n)," *ISSCC Proc.*, pp. 560-561, Feb., 2007.

[2] Y. Palaskas, *et al*, "A 5-GHz 108-Mb/s 2x2 MIMO transceiver RFIC with fully integrated 20.5-dBm P_{1dB} power amplifiers in 90-nm CMOS," *IEEE J. Solid-State Circuits*, vol. 41, no. 12, pp. 2746-2756, Dec. 2006.

UC Irvine Center For Pervasive Communications and Computing

Graduate Fellowship Progress Report Winter 2008

April 23, 2008

Project Name: Adaptive Equalization of Multimode Fiber Channels in $0.13\mu m$ CMOS
CPCC Affiliate Professor: Michael Green
Mailing Address: 544 Engineering Tower, Irvine CA 92697-2625
Phone No.: 949-824-1656 **E-mail:** mgreen@uci.edu
Student Fellowship Recipient: Mahyar Kargar

Introduction

With increasing data rates and link distance in fiber-optic systems, the transmission path becomes severely limited by fiber non-idealities, especially dispersion. Intersymbol interference (ISI) is a fundamental limiting factor in band-limited communication links. In particular, in multimode optical fiber, which are the dominant fiber type in local area network (LAN) links like 10Gb/s Ethernet,the ISI is mainly due to modal dispersion. Electronic dispersion compensation (EDC) is used to combat this ISI in short-distance fiber links. Use of adaptive equalizers as an EDC method is known to make the data communications over short ranges of the MMF possible. In this project a high-speed adaptive DFE is designed to combat the ISI caused by the band-limited MMF channel.

Summary of Accomplishments

The design of feed-forward filter (including the DLL and gain control loop) and the adaptive feedback filter (including high-speed slicer and DFF's) has been completed in $0.13\mu m$ CMOS. LMS algorithm is implemented to adaptively change the feedback filter coefficients using an analog integrator and a Gilbert multiplier.

The project is in the layout and integration mode now. The building blocks of the feed-forward and feedback filters have been laid out and the results have been verified with post-layout simulations.

The LMS circuit block with Gilbert multiplier and integrator has been laid out and verified. The 10Gb/s CDR design is almost completed.

A 10Gb/s binary Alexander phase detector for the CDR loop has been designed using high-speed DFFs and symmetric XOR circuits. The phase detector has been laid out and post lay out extracted simulations have been performed to verify the performance. Top level CDR loop simulations using extarcted phase detector and ideal VCO have been performed to verify the CDR locking behavior.

Ongoing Work

1. Verification of the feed-forward filter with post-layout simulations on extracted blocks after layout.
2. Verification of the feedback filter with post-layout simulations extracted blocks after layout.
3. Verification LMS circuit convergence properties using transistor level post-layout simulations.
4. Top level simulation of the 10Gb/s CDR with extracted VCO verifying the locking behavior and performance.
5. Layout and post-layout extraction of the remaining blocks in the CDR.
6. Considering different $0.13\mu m$ CMOS RF design kits like STMicroelectronic's HCMOS-9RF or IBM's 8RF-DM instead of Jazz ca13.

Progress Report on Temperature and Error Aware Memory Design: Winter 2008

Amin Khajeh Djahromi, Advisor: Professor Ahmed Eltawil
Center for Pervasive Communications and Computing
Department of Electrical Engineering and Computer Science
The Henry Samueli School of Engineering
University of California, Irvine
Irvine, California 92697-2625
Email: akhajehd@uci.edu

Abstract— **Memories are increasingly dominating Systems on Chips (SoCs) designs. Hence, they represent a majority share of the total system's power dissipation. Shrinking device geometries and increasing power dissipation have resulted in high operating temperatures of designs. SoCs often have on-chip temperature gradients of up to 50°C. Conventionally, designers increase (overdrive) the supply voltage (V_{dd}) to increase the reliability of the memories which in turn increases their power dissipation. On the contrary, by considering the effect of temperature on memories, we observe that reducing V_{dd} can help improve both the reliability and the power dissipation. In this report we propose Temperature-and Error-Aware Memory Design (TEAM) which optimizes embedded memory design while considering both thermal and error issues. Using TEAM, designers can optimize memories' power dissipation while maintaining both performance and error metrics. Our experimental results indicate that thermal unaware estimation of probability of error can be off by at least two orders of magnitude and up to five orders of magnitude.**

I. Introduction

Process scaling has enabled systems to offer much higher computational power and performance at the expense of rising power consumption and operating temperatures. Higher operating temperatures have many adverse effects on the design such as: need for expensive cooling mechanisms, increased leakage power, reduced interconnect lifetime, accelerated electromigration, increased cell delay, and increased probability of errors in memories and logics [3]. In this report we focus on the effect of temperature on reliable operation of memories. This work can also be applied on logic circuits because they exhibit a similar change in behavior due to temperature. Some systems do not support any data error tolerance such as the instruction cache in a processor. however, many Systems on Chip (SoC) designs have algorithms and techniques which support error resilience up to a predefined limit. For example, communication systems operate under harsh wireless conditions and low SNR (signal to noise ratio). It is imperative to incorporate error correction schemes such as the Viterbi Algorithm [4] or Turbo codes in the system. But these error correcting mechanisms consume large amount of power. SoC designers aim to achieve the best possible performance (both speed and probability of errors) while minimizing the total power consumption. There is an intrinsic trade-off between the power consumption and the error resiliency of a design. Conventionally, designers increase the supply voltage V_{dd} to increase the reliability of the memories (reduce the probability of errors). But this comes at the cost of increased power dissipation. Temperature increases the cell delay which causes the probability of errors in a memory to increase [2]. An increase in V_{dd} also increases the dynamic power dissipation of the memory cell which raises the temperature of the memory. Thus there are two conflicting phenomena: increase in V_{dd} which reduces memory errors and increase in temperature which increases memory errors. Another factor which influences the dynamic power dissipation is frequency. Increase in frequency increases both dynamic power dissipation and the probability of errors in memory. Temperature has a very significant impact on the leakage power dissipation. In fact there exists a positive feedback loop between temperature and leakage power. All the above relationships motivated us to comprehensively examine the aggregate effect of V_{dd}, frequency, leakage power, and temperature on the reliability of memories. In this report we present a Temperature- and Error- Aware Memory Design (TEAM) framework. During the Winter 2008, we studied the effect of the temperature and voltage scaling on the embedded memory stability. The main contribution of our work is the observation that when we consider the thermal aspect during memory design reducing V_{dd} (from the over-drived V_{dd}) can help improve both the reliability and the power dissipation, which is contrary to the conventional practice.

II. Sensitivity of Errors

Fig. 1 shows how errors in memory are affected by different parameters. As the operating frequency is increased the probability of memory errors increase because it enforces tighter bounds on the time allowance for memory accesses. Increase in V_{dd} reduces the cell delay and thus causes the errors to decrease. The errors in memories increase along with the rise in temperature because of increase in the cell delay. These are not the only relationships that effect memory errors. From Fig. 1 we also examine other interrelationships at work. The dynamic power dissipation in memory cell increases with increase in both frequency (α f) and V_{dd} (α V^2_{dd}). The leakage power, on the other hand, increases only with V_{dd} (α $e^{-\beta V_{dd}}$, β >1). Both dynamic power and leakage power dissipation determine the operating temperature. Leakage power dissipation of a cell is known to increase super-linearly with increase in temperature. As temperature increases, the leakage power dissipation increases which further elevates the temperature. This 'positive feedback loop' between temperature and leakage power stabilizes when steady state operating temperatures have been reached at which state all the dynamic and leakage power dissipation is transferred to the environment by the package [1]. Thus the list of parameters that affect the probability of errors in memory (or logic) is as follows: V_{dd}, frequency, temperature, leakage power, and dynamic power. A comprehensive approach to memory/logic design must consider these relationships

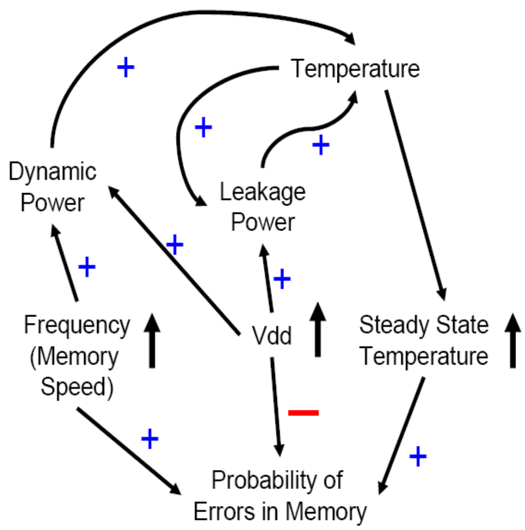

Figure 1, Sensitivity of Memory Errors to Various Parameters

III. Simulation Results

For our experiments we use HotSpot [6] tool to determine the temperature of memory for different supply voltages. Because of super linear dependency of leakage on temperature we have coupled leakage power models with HotSpot. Rise in leakage power raises the temperature which in turn affects leakage power, and we have also modeled this positive feedback loop in our framework. After obtaining expected temperature values for different V_{dd}s we run a HSPICE simulation in order to calculate the probability of failure. This HSPICE simulation uses 65nm Predictive Technology Models (PTM) [7]. Fig. 2 shows the relationship between the probability of error and the V_{dd} for a cell with maximum allowed time of 65ps. The curves show the probability of error for the estimated temperature profile (using the dependencies shown Fig. 1) and at two corner case temperatures of 25^{o}C and 105^{o}C. Since we are only considering $6\sigma_{Vth}$ variation for each transistor, the smallest probability of error that we can calculate is 10^{-18} [5]. From the figure, we observe that the probability of error is significantly higher at higher temperatures. For example, at V_{dd} = 0.9v the probability of error is of the order of 10^{-8} at 25^{o}C versus 10^{-1} at 105^{o}C. However, when we estimate the probability of error while considering the interrelationships between V_{dd} and temperature, we observe that the probability of error is of the order of 10^{-6} at V_{dd} = 0.9v. These observations quantify the effect of temperature on the probability of error in a memory. We also observe that for 105^{o}C, an inversion in trend of probability of error occurs at V_{dd} = 1.1v (marked χ). Because of dominance of the effect of temperature (which increases the probability of error) we observe that an increase in V_{dd} fails to reduce the probability of error. We observe similar phenomenon for the curve for estimated temperature profile (marked γ). As V_{dd} increases, the temperature increases very steeply because of which we observe that the probability of errors increase. This demonstrates that an increase in V_{dd} does not guarantee a reduction in the probability of error because of the effect of temperature described in the previous sections.

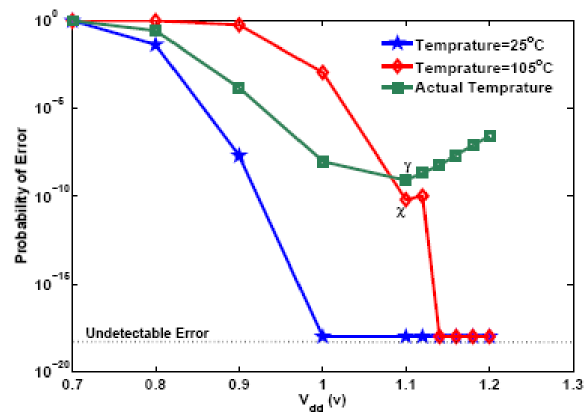

Figure 2, Probability of Error for Different Temperature Profiles

IV. Future Work

In subsequent quarters we intend to extend our study to identify analytic equations that can help the designer predict stable points of operation with minimum energy for a given probability of error that can be tolerated by the system.

References

[1] A. Gupta et al., "A System Level Leakage-Aware Floorplanner for SoCs,"Proc. of ASP-DAC, 2007.

[2] K. Banerjee et al., "Analysis of Non-Uniform Temperature-Dependent Interconnect Performance in High Performance ICs," Proc. of Design Automation Conference, 2001.

[3] V. De et al., "Technology and design challenges for low power and high performance," Proc. of Intnl. Symp. on Low Power Electronics and Design, 1999.

[4] A. Viterbi et al., "Error bounds for convolutional codes and an asymptotically optimum decoding algorithm," IEEE Transactions on Information Theory, April 1967.

[5] A. Djahromi et al., "Cross Layer Error Exploitation for Aggressive Voltage Scaling," International Symposium on Quality Electronic Design, 2007

[6] K. Skadron et al., "An Improved Block-Based Thermal Model in HotSpot-4.0 with Granularity Considerations," Proceedings of the Workshop on Duplicating, Deconstructing, and Debunking, 2007.

[7] Predictive Technology Model (PTM): http://www.eas.asu.edu/~ptm/

A Framework of a High-level Power Estimation for A Network-on-Chip Router: WINTER 2007

Seung Eun Lee, Advisor: Nader Bagherzadeh
Center for Pervasive Communications and Computing
University of California-Irvine
Email: seunglee@uci.edu

***Abstract*—In Winter 2008, we derived a high-level power macro model for an adaptive router, which allows network power to be readily incorporated into simulation infrastructures, providing a fast and cycle accurate power profile to enable power optimization for multi-processor.**

I. Introduction

Although today's processors are much faster and far more versatile than their predecessors using high-speed operation and parallelism, they also consume a lot of power. Moreover, an interconnection network dissipates a significant fraction of the total system power budget. Therefore, interconnection network must be designed to be power aware. It is desirable to get detailed trade offs in power and performance early in the design flow, preferably at the system level. However, there is limited tool support available for power analysis of an interconnection network.

In Winter 2008, we developed a framework for router power analysis that uses the number of flits passing through a router as the unit of abstraction in order to speed up of network simulation because the detailed modeling at the low level abstraction can further exacerbate the complexity of simulator. When validated against gate level simulation, our power model derives power profiles that match closely with that of gate level analysis. The high level power macro model allows network power to be readily incorporated into simulation infrastructures, providing a fast and cycle accurate power profile, to enable power optimization such as power-aware compiler, core mapping, and scheduling techniques for multi-processor. By evaluating the effect of different core mappings using SPLASH-2 benchmark, how power analysis can facilitate power optimization of NoC was demonstrated.

II. Power Macro Model

We created a power macro model for a single router [1]. From the simulation results, two important conclusions were drawn: (1) different payload affects differently the power because dynamic power is proportional to the switching activity of gates ($P = \frac{1}{2}\alpha C V_{dd}^2 f$, with f the clock frequency, α the switching activity, C the switch capacitance, and V_{dd} the supply voltage). (2) the state of each outgoing port has a close relation to the overall power. In particular, state transition of outgoing port has a noticeable effect on its power consumption. Based on these observations, the power consumption of the router can be given as:

$$\hat{P} = \alpha_0 + \alpha_H \cdot \psi_H + \alpha_S \cdot \psi_S + \alpha_{\Delta S} \cdot \psi_{\Delta S} \qquad (1)$$

where ψ_H is Hamming distance of outgoing flits; ψ_S is the number of outgoing ports passing body flits; and $\psi_{\Delta S}$ is the number of state transitions of outgoing ports.

Figure 1 shows a snapshot of the power waveform generated by the power macro model (solid line) and gate level simulation (dotted line) using PrimeTime for a router located at (2,2) in a $4\quad 4$ mesh network. The L3 power waveform is very close to the gate level power waveform, while the L2 power waveform shows less detailed estimation. The power model of the L3 allows extremely accurate power estimation with more than 10000   speed up over PrimeTime based estimation. As can be seen, the power estimates from the power model are highly correlated to the actual power consumption. Even though sporadic peaks are present, they do not affect the global behavior of the power model. The experimental results have confirmed the reliability of our power model, being the average absolute cycle error with respect to PrimeTime analysis within 5%. The power model allows desgner simulate various strategies to observe their influence on power quickly, which is not practically feasible with gate level simulation.

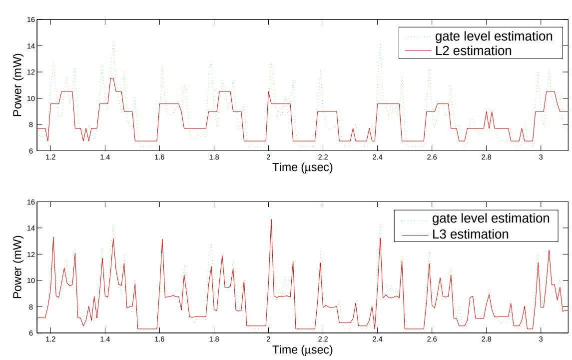

Fig. 1. Predicted and measured power waveforms at level 2 and level 3

References

[1] S. E. Lee, J. H. Bahn, and N. Bagherzadeh, "Design of a feasible on-chip interconnection network for a chip multiprocessor (cmp)," in *SBAC-PAD'07: Proceedings of the 19th International Symposium on Computer Architecture and High Performance Computing*, 2007.

UC IRVINE CENTER FOR PERVASIVE COMMUNICATIONS AND COMPUTING

CPCC Fellowship Spring Quarter Progress Report, May 2008

Project1 Name: Charge pumped wordline driver foe voltage scalable process variation aware caches
Project2 Name: Word Level remapping for improving fault tolerance.

Graduate Student: Mohammad A Makhzan EECS (on CPCC Fellowship for SQ 2008)
CPCC Affiliate Professors: Fadi J. Kurdahi and **Ahmed Eltawil**

Project1 overview:

This project was initiated following our previous studies on parametric defects in the result of process variation. As technology migrates to smaller geometries process variation, due to physical limitations of processing technologies, will increasingly affect the behavior of the memory cells. Considering the structure of the memory arrays and their dense arrangement (minimum geometry transistor sizes), the defect density is therefore much higher in the memory structures compare to logic.

In this project we developed a process variation aware architecture. In our proposed memory, the wordline driver is altered to allow selective charge pumping on weak wordlines (wordlines containing cells that are severely affected by process variation). Our studies show ~35% improvement in access time, ~40% improvement in write time from/to cells in the weak wordlines that are activated using our proposed architecture. Process variation results in a Gaussian distribution of access times. The new architecture controls the process variation in two ways. It shifts the mean access time to smaller values, and also it reduces the standard deviation from mean access time across all cells. The area overhead of the architecture is negligible (~1% of the memory size). The ability to tolerate higher number of defects makes the new architecture a preferred candidate for voltage scaling. This study has resulted in the submission of following papers for publication.

Publications:

1- **M. Makhzan, H. Houmayoun, F. Kurdahi, A. Eltawil "Process Variation Aware Wordline Driver for Low Voltage Operation" ICCAD 2008 (Submitted)**
2- **M. Makhzan, H. Houmayoun, F. Kurdahi, A. Eltawil "Process Variation Aware Aggressive Voltage frequency scaling for Embedded Processors." MICRO 2008 (Under preparation)**

We are also working on preparing a journal paper for submission to TVLSI

Project2 overview:

This project was initiated based on understanding that single bit faults (stuck at ones “SA1” and stuck at 0 “SA0”) consist the majority of defects in the memory structures. In addition as the technology scales the parametric defects (discussed in the overview of the previous project) will increase exponentially dominating the defect density. However process variation defects are random and uniform in nature and they could all be looked at as single bit faults. Our proposed remapping architecture allows finer granularity when remapping the defects to the redundancy section and replaces one word (32 bits) rather than an entire row in redundant rows. The proposed remapping technique is only applicable to banked memories. In order to avoid multi cycle access for a block (that should be read in one cycle) the remapping is done to the redundancy section of the next bank. This project has resulted in the following publications.

1- **M. Makhzan, H. Houmayoun, F. Kurdahi, A. Eltawil “Architectural and Algorithm level Fault Tolerant Techniques for Low Power High Yield Multimedia Devices” SAMOS 2008**
2- **M. Makhzan, H. Houmayoun, F. Kurdahi, A. Eltawil “Voltage Scaling for Caches Utilizing Dynamic Word Level Remapping ” CASES 2008 (submitted)**

A journal paper on word level remapping is being prepared.

Optimal Rate Allocation for Video Transmission over a Wireless Channel

Negar Nejati, Advisor: Hamid Jafarkhani
Center for Pervasive Communications and Computing
Department of Electrical Engineering and Computer Science
The Henry Samueli School of Engineering
University of California, Irvine
Email: nnejati@uci.edu

***Abstract*—In this paper we introduce an analytical expression for the expected distortion of a single layer encoded video bit-stream. Based on the expected distortion model we propose a distortion-optimal Unequal Error Protection (UEP) technique to transmit such video bit-stream over wireless tandem channel. The proposed method allocates the total transmission budget unequally to the different frames of a video bit-stream to protect the bit-stream against both bit errors caused by fading and packet erasures caused by network buffering. We have compared this technique with two other UEP methods as well as one-dimension Equal Length Protection (ELP) scheme. The evaluation results for different choices of packet sizes, available budgets and channel conditions show that the proposed method outperforms the other schemes.**

I. Introduction

Recently several transmission techniques have been proposed to improve the level of quality of transmitted video over the packet loss channels. Wireless channels are identified by temporally correlated tandem loss patterns which appear in the form of bit errors related to fading and packet erasures related to network layer buffering. But the effect of bit errors related to fading is not considered in most of the literature works. In this paper we propose a low complexity optimal-distortion rate allocation method to protect the single layer encoded video bit-stream against bit errors and packet erasures. First we introduce an analytical distortion model for single layer video stream transmitted over a tandem channel. Figure 1 shows a sample result of our experiment for Foreman sequence.

Using this model and MoMuSys video code implementing MPEG4 standard, we defined and solve a distortion-optimal rate-allocation for video transmission over a tandem channel. We have assumed that the encoded video bitstream is packetized with fixed packet size and each frame is protected with one-dimensional RS code. Our coding scheme also interleaves the symbols to better cope with the temporally correlated loss observed over the tandem channels of interest.

We have compared the proposed method, OSL, with two other UEP methods. LDO method assigns parity budget to each frame based on the ratio of the distortion that their loss will cause to the total distortion of that GOP being lost and the other scheme ULP which was proposed previously in [1], assembles the video packets of each GOP into several blocks of packets (BOP). The first BOPs contain the video packets with higher priority compared to the latter BOPs and therefore more FEC packets are assigned to them. The simulation results are provided in the next section.

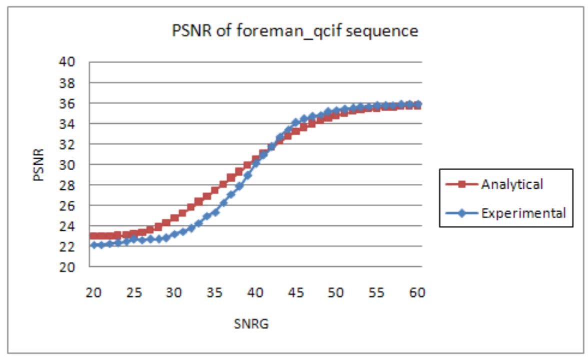

Fig. 1. A comparison of analytical and experimental distortion results of Foreman sequence.

II. Simulation Results

In this section, we provide the results of proposed technique OSL, for different channel conditions and total budgets as well as the compared results of OSL scheme with ULP, LDO and Equal Loss Protection (ELP) methods. In our experiments, we use a tandem channel introducing both bit errors and packet erasures. The video codec used in this work is MoMuSys [2] [3] implementing MPEG4 standard. We apply transition probabilities of $\gamma = 0.99875$ and $\beta = 0.875$ for the GE chain used for bit errors. The average burst lengths associated with these values are 800 and 8, respectively. We choose an SNR range of $[4, 60]$dB for GOOD state of the GE chain and set SNR_G=10 SNR_B to differentiate between the two states.The G chain used for packet erasures has the same γ as the GE chain and its β parameter changes in the range of $[0.87625, 0.995]$. We report the results of our experiments with Foreman sequence. The total budget and packet size are assumed to be fixed for all of the transmission methods. The results of 114% total transmission budget applied to the single layer encoded bitstream of Foreman sequence in qcif format with packet size equal to 64 bytes is presented in Fig. 2. Fig. 3 shows the improvement of quality of received video using the proposed technique by increasing the total transmission budget. The comparison results of OSL method and LDO

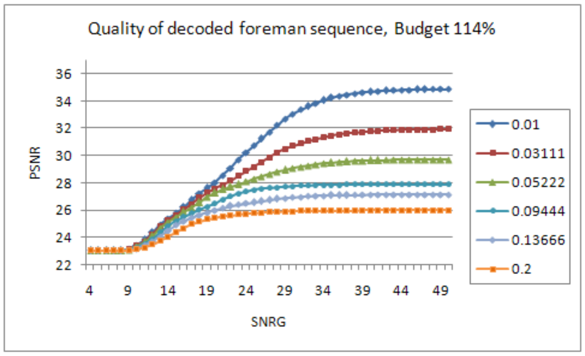

Fig. 2. Results of Proposed scheme in different channel conditions with 114% budget.

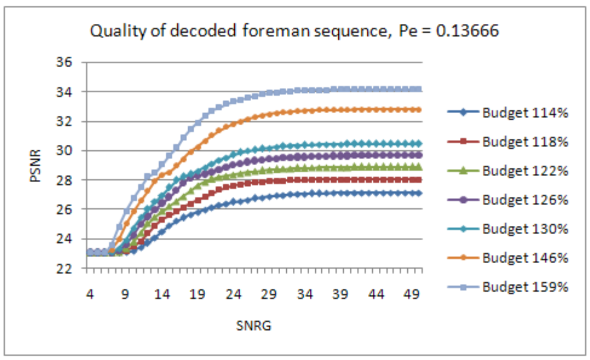

Fig. 3. Results of Proposed scheme for different budgets in different bit error conditions.

scheme are shown in Fig. 4 and Fig. 5. In Fig. 4 the total transmission budget is fixed and equal to 114% while in Fig. 5 the results are shown for different budgets while the packet loss probability of channel is assumed to be fixed. As the

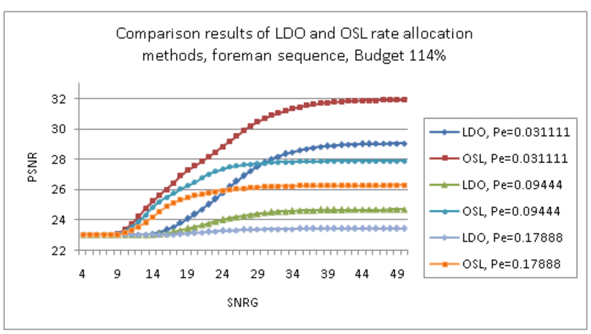

Fig. 4. Comparison results OSL and LDO scheme in different channel conditions with 114% budget.

ULP scheme was proposed for the packet erasure channels with no bit errors, we compared the proposed OSL technique with ULP and ELP schemes in the channel conditions where there is no bit errors. Fig. 6 shows these comparison results

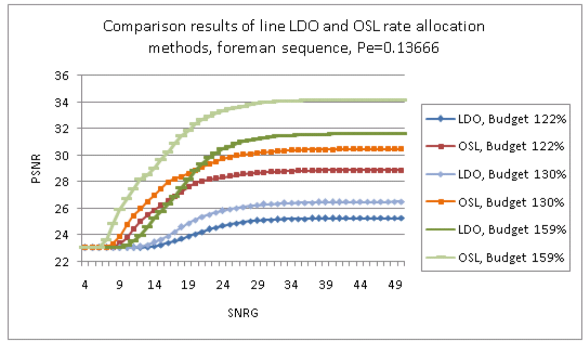

Fig. 5. Comparison results of OSL and LDO scheme for different budgets in different bit error conditions.

for different parity rates. The results show that the proposed

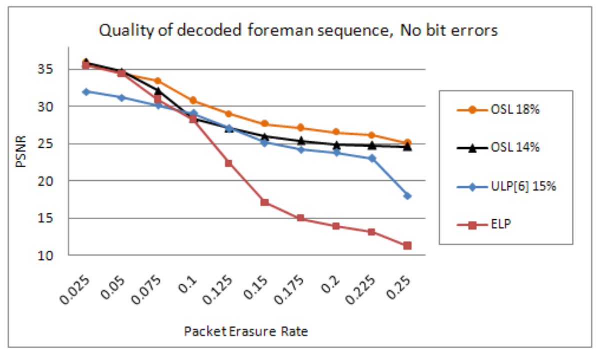

Fig. 6. Comparison results of OSL, ULP and ELP schemes for packet erasure channel.

technique can improve the quality of received video specially in high packet erasure rate channels.

REFERENCES

[1] X. Y. et al., "Unequal loss protection for robust transmission of motion compensated video over the internet," *Signal Process. Image Communications*, March 2003.

[2] "General project information, the momusys web site," *available at http://www.tnt.uni-honnover.de/project/eu/momusys/.*

[3] "Final report on standardisation activities, MoMuSys Public Deliverable," *available at http://www.tnt.uni-honnover.de/project/eu/momusys/doc/mom-docs.html.*

UC IRVINE CENTER FOR PERVASIVE COMMUNICATIONS AND COMPUTING
Graduate Fellowship - Progress Report for Winter 2008

Ph.D. Student: Hulya Seferoglu
Date: April 23, 2008
CPCC Affiliate Professor: Athina Markopoulou

Overview: During winter 2008, we completed our work on the problem of *network coding for video streaming*. Simulations on the network coding algorithms, NCV and NCVD proposed in [1] are completed using the simulator we have written on Glomosim simulation environment, [2]. This work including all the proposed algorithms, baselines, and extended simulation results are now submitted for journal publication, [3]. In this quarter, we have explored a new problem *joint rate allocation and scheduling for network coding over wireless.*

Network Coding for Video: Network coding is an emerging area [4] that started with [5, 6] in the context of multicast networks, stating that if intermediate nodes are allowed to perform simple operations on incoming packets, then the network can achieve the min-cut throughput to each receiver. Of particular interest to our work is [7], which demonstrated that network coding can increase throughput over a broadcast medium, by mixing packets from different flows into a single packet, thus increasing the information content per transmission. Our key insight in this project is that, when the transmitted flows are video streams, network codes should be selected so as to maximize not only the network throughput but also the video quality. During winter 2008, we completed the simulations of the proposed network coding schemes, *Network Coding for Video (NCV*), and NCVD, [1] and submitted the journal paper of this work for publication, [3].

Joint Rate-Allocation and Scheduling for Network Coding over Wireless: Resource allocation problems in both wired and wireless networks are important to be able to use networks efficiently and to allocate resources fairly to competing users. Most of the work in this area follows the approach of f Kelly et. al., [8]. Recently, there is increasing interest to resource allocation problems in wireless networks, [9], especially on resource allocation for multi-hop wireless. This problem is challenging due to broadcast nature of wireless. It becomes more challenging when network coding is employed. The example in Fig. 1 shows our motivation. In this figure, node A and node B are talking to each other over a relay R. It is wireless environment where A and B do not hear each other. Let us suppose that node A is transmitting at rate r_1 and node B is transmitting at rate r_2, and assume that node R is performing a basic network coding operation (XORing of packets from node A and node B) and broadcasting. If $r_1 = r_2$, R will combine two packets coming from A and B at a time. Therefore, the relay will transmit at a rate $r_3 = r_1 = r_2$. When $r_1 > r_2$, relay node will transmit at a rate $r_3 = r_1$, because the relay node should serve all the packets from node A with rate r_1 and add (XOR) the packets coming from node B to these packets. Therefore, the relay node should transmit at a rate $r_3 = \max(r_1, r_2)$. This example shows that when network coding is used, an intermediate node may transmit at lower rates than the summation of all the rates incoming to this node. In rate allocation models, transmission data rate at each node and its upper bound due to channel capacity determines the constraints of the model. Our goal is (i) to formulate the optimal rate allocation problem by taking into account the effect of network coding on transmission rates per node and (ii) to develop a distributed solution to the proposed model.

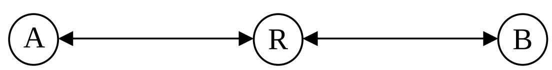

Figure 1: Cross topology with two nodes talking to each other

In wireless networks, it is shown that scheduling should be decided jointly with rate allocation to achieve targeted achievable capacity, [9]. A scheduling mechanism decides on which node should transmit at a given time. This problem is interesting from the point of network coding, because intermediate nodes do not directly relay packets anymore, instead they should wait for some packets to be able to perform network coding. The problem is to make a decision on how long intermediate nodes should wait and how the nodes should be coordinated to make the distributed scheduling possible considering network coding. Our goal is to consider the scheduling problem jointly with the rate allocation problem.

Future Directions:

In the spring quarter, we will continue to work on joint rate-allocation and scheduling problem for network coding over wireless networks. Specifically future work on this topic includes developing an optimization model, proposing a distributed solution to this model, showing the optimality and stability of the solution, and conducting extensive simulation results.

References:

[1] H. Seferoglu, A. Markopoulou, "Opportunistic Network Coding for Video Streaming over Wireless," *in Proc. of Packet Video 2007*, Lausanne, Switzerland, Nov. 2007.
[2] Glomosim webpage, *http://pcl.cs.ucla.edu/projects/glomosim/*.
[3] H. Seferoglu, A. Markopoulou, "Opportunistic Media-Aware Network Coding for Video Streaming over Wireless Networks," *submitted to Transactions on Multimedia.*
[4] The network coding webpage, *http://www.netcod.org.*
[5] R. Ahlswede, N. Cai, S. R. Li, and R. W. Yeung, "Network Information Flow," *in IEEE Transactions on Information Theory*, vol. 46, pp. 1204-1216, 2000.
[6] S-Y. R. Li, R.W. Yeung,, and N. Cai, ``Linear network coding,'', *in IEEE Trans. on Information Theory*, Vol. 49, 2003.
[7] S. Katti, H. Rahul, W. Hu, D. Katabi, M. Medard, J. Crowcroft, "XORs in The Air: Practical Network Coding," *in Proc. of ACM SIGCOMM*, 2006.
[8] F. Kelly, A. Maulloo, D. Tan, "Rate Control for Communication Networks: Shadow Prices, Proportional Fairness and Stability," *Journal of the Operations Research Society*, vol. 49 (3), pp. 237 – 252, 1998.
[9] X. Lin, N. B. Shroff, R. Srikant, "A Tutorial on Cross Layer Optimization in Wireless Networks," *IEEE Journal on Selected Areas in Communications*, vol. 24 (8), pp. 1452 – 1463, 2006.

Progress Report on MIMO System Design With Receive Polarization Diversity: Winter 2008

Volkan Sevindik, Advisor: Ender Ayanoglu
Center for Pervasive Communications and Computing
Department of Electrical Engineering and Computer Science
The Henry Samueli School of Engineering
University of California, Irvine
Irvine, California 92697-2625
Email: vsevindi@uci.edu

I. Introduction

Diversity techniques are widely used to combat the effects of wireless fading channels. The replicas of the same information bits are received in the receiver. It is less likely that all replicas of the same information will be in deep fading simultaneously. The most commonly used diversity techniques [6] are *frequency diversity* where signals are transmitted on different frequencies, *time diversity* where signals are transmitted at different times, *space diversity* [1] where signals are transmitted and/or received by multiple antennas. *polarization diversity* [2] where signals are transmitted/received with different polarization directions of antennas, *angle diversity* where signals are received by directional antennas.

The most obvious approach to diversity is the use of spatially separated antennas (*space diversity*). *Space diversity (antenna diversity)* is one of the key techniques to reduce the effect of multipath fading in wireless systems [1] - [5]. One can use multiple antennas at the transmitter/receiver which is called *transmit diversity* and *receive diversity* respectively.

II. Problem Definition

In MIMO system, in order to fully exploit diversity, spacing between adjacent antenna elements at the transmitter and receiver sides should be at least 10 - 15 wavelengths and 3 - 5 wavelengths respectively. From implementation point of view, it is hard to have multiple antennas with enough spacings at wireless handheld devices which are getting smaller day by day.

Therefore, we focus on designing MIMO system that implements polarization diversity at only the receiver side. In other words, we use uni-polarized antennas at the transmitter side, but dual-polarized antennas at the receiver side because of the space limitations. The channel model is different when the system employs polarization diversity. In our work, we will use the channel model given in [2], which is

$$\mathbf{H} = \sqrt{\frac{K}{1+K}}\bar{\mathbf{H}} + \sqrt{\frac{1}{1+K}}\tilde{\mathbf{H}} \qquad (1)$$

In the case of *polarization diversity*, the channel matrix $\mathbf{H}$ can be decomposed into fixed and variable component as it is seen from channel definition. In this definition, K specifies fading characteristic of the channel that takes value between 0 and 10. K=0 corresponds to the pure *Rayleigh* fading and K $\neq$ 0 corresponds to the *Ricean* Fading.

In [2], the performance of Alamouti scheme is analyzed under receive antenna and transmit antenna polarization diversity. The input-output relation is given as [2],

$$\widetilde{r}_i = \sqrt{E_s}||\mathbf{H}||_F^2 s_i + \widetilde{n}_i, \qquad i = 0,1 \qquad (2)$$

where $\widetilde{r}_i$ is the scalar processed received signal corresponding to transmitted symbol s_i (i=0,1), and $\widetilde{n}_i$ is a scalar zero-mean complex gaussian noise with variance $\varepsilon\{|\widetilde{n}_i|^2\} = ||\mathbf{H}||_F^2\sigma_n^2$, and $||\mathbf{H}||_F^2$ is the squared Frobenius norm of the channel matrix [2]. For 2 Tx-2Rx MIMO system, the elements of $\mathbf{H}$ matrix are given as,

$$\mathbf{H} = \begin{bmatrix} h_{00} & h_{01} \\ h_{10} & h_{11} \end{bmatrix} = C_1 \begin{bmatrix} \bar{h}_{00} & \bar{h}_{01} \\ \bar{h}_{10} & \bar{h}_{11} \end{bmatrix} + C_2 \begin{bmatrix} \tilde{h}_{00} & \tilde{h}_{01} \\ \tilde{h}_{10} & \tilde{h}_{11} \end{bmatrix} \qquad (3)$$

The transmit and receive correlation coefficients, t and r, respectively are defined as,

$$r = \frac{E\{\widetilde{h}_{1,1}\widetilde{h}_{0,1}^*\}}{\sqrt{\alpha}} = \frac{E\{\widetilde{h}_{1,0}\widetilde{h}_{0,0}^*\}}{\sqrt{\alpha}} \qquad (4)$$

$$t = \frac{E\{\widetilde{h}_{1,1}\widetilde{h}_{1,0}^*\}}{\sqrt{\alpha}} = \frac{E\{\widetilde{h}_{0,1}\widetilde{h}_{0,0}^*\}}{\sqrt{\alpha}} \qquad (5)$$

where α is polarization discrimination factor of dual-polarized antennas. We assume that same polarized directions are independent from eachother,

$$E\{\widetilde{h}_{1,1}\widetilde{h}_{0,0}^*\} = E\{\widetilde{h}_{0,1}\widetilde{h}_{1,0}^*\} = 0. \qquad (6)$$

III. Simulation Results

The simulations results below show BER performance comparison for Alamouti space-time block code for different MIMO systems under correlated channel conditions. We made monte carlo simulations in order to see the effects of polarization diversity. We used BPSK modulation and sent 1000 packets each of which consists of 1000 bits and symbol errors were counted. In the receiver ML decoding is used and we have perfect channel knowledge. MRC (maximal ratio combining) is used in order to produce the estimates of transmitted symbols. The SNR was defined as $10\log(2E_s/\sigma_n^2)$ for 2 Tx MIMO system.

Figure 1 shows the BER performance comparison of Alamouti's method for 2Tx-1Rx and 2Tx-2Rx scenarios with Maximal Ratio Receive combining scheme. For theorical results of Alamouti scheme, pairwise error probability formula is given in [5].

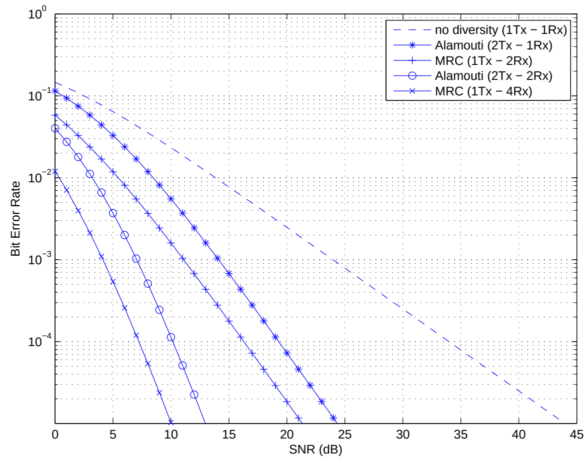

Fig. 1. The BER performance of Alamouti scheme for 2Tx-1Rx MIMO system in Rayleigh fading

Figure 2 shows the SER performance comparison of Alamouti's method for 2Tx-1Rx and 2Tx-2Rx scenarios with 4Tx-2Rx and 4Tx-1Rx scenarios for which rate 1/2 orthogonal space-time block code is used.

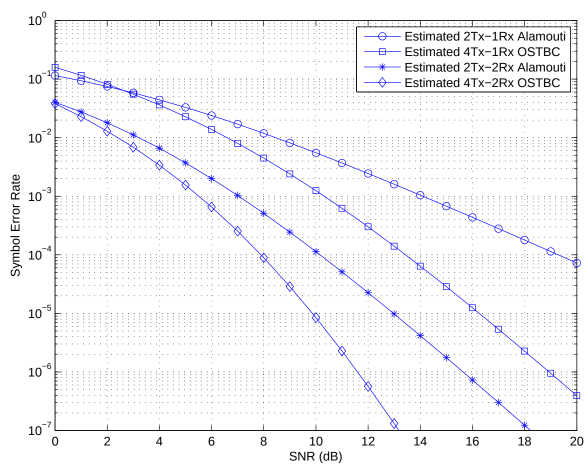

Fig. 2. Symbol error rate comparison of Alamouti scheme with 4Tx - 2Rx and 4Tx - 1Rx channel scenarios

Figure 3 shows the SER performance comparison of Alamouti's method for 2Tx-1Rx, and under polarization diversity with system parameters $\alpha = 0.4, t = 0, r = 0.3$

IV. Conclusion and Future Work

As it is seen from the Figure 3, when the MIMO system uses only transmit diversity, its performance will be better than

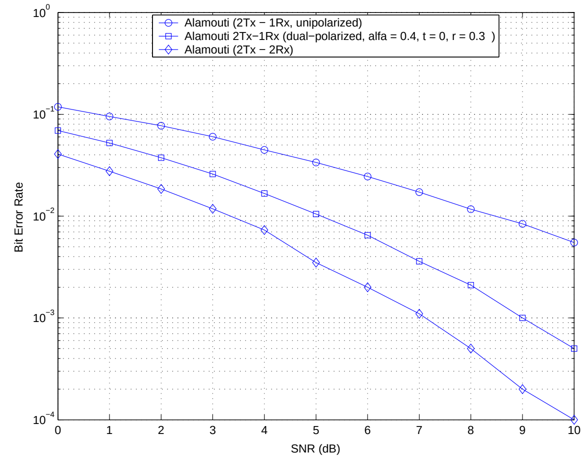

Fig. 3. Symbol error rate comparison of Alamouti scheme with 4Tx - 2Rx and 4Tx - 1Rx channel scenarios

2Tx-1Rx system. The system performance highly depends on the system parameters. The degree of discrimination between orthogonal polarized directions has profound effect on bit error rate (BER) performance of the system. In case of polarization diversity, there is correlation between the information symbols sent from the receiver, so using ML receiver (hard decoding) does not exploit the correlation between symbols for better symbol decisions. Therefore, we consider using soft decoding techniques at the receiver in order to use the correlation information in symbols.

References

[1] Alamouti, S. M., "A Simple Trannsmit Diversity Technique for Wireless Communications", *IEEE J. Select. Areas Commun.*, Vol. 16, No. 8, pp. 1451-1458, October 1998.

[2] Nabar, R. U., H. Bölcskei, V. Erceg, D. Gesbert and A. J. Paulraj, "Performance of Multiantenna Signaling Techniques in the Presence of Polarization Diversity", *IEEE Trans. Signal Process.*, Vol. 50, No. 10, pp. 2553-2562, October 2002.

[3] Nabar, R. U., H. Bölcskei, V.Erceg, D. Gesbert and A. J. Paulraj, "Diversity and Outage Performance in Space-Time Block Coded Ricean MIMO Channels", *IEEE Trans. Wireless Commun.*, Vol. 4, No. 5, pp. 2519-2532, September 2005.

[4] Paulraj, A. J., D. A. Gore, R. Nabar and H. Bölcskei, "An Overwiev of MIMO Communications -A Key to Gigabit Wireless", *Proc. IEEE*, Vol. 92, No. 2, pp. 198-218, February 2004.

[5] Tarokh, V., N. Seshadri and A. R. Calderbank, "Space-time Codes for High Data Rate Wireless Communication:Performance Criterion and Code Construction", *IEEE Trans. Inform. Theory*, Vol. 17, No. 3, pp. 451-460, March 1999.

[6] Tarokh, V., H. Jafarkhani and A. R. Calderbank, "Space-time Block Coding for Wireless Communications:Performance Results", *IEEE J. Select. Areas Commun.*, Vol. 16, No. 8, pp. 1451-1458, October 1998.

[7] Uysal, M. and C. Georghiades, "On the error performance analysis of space-time trellis codes: an analytical framework", *Proc. IEEE WCNC*, pp. 99-104, July 2002.

Progress Report Winter 2008: Interference Alignment and Degrees of Freedom of Interference Channels under Channel Estimation Error

S. Surendran
Under the supervision of Prof. Syed A. Jafar
Center for Pervasive Communications and Computing
Department of Electrical Engineering and Computer Science
University of California, Irvine
Irvine, California, 92697, USA
Email: ssurendr@uci.edu

***Abstract*— Interference alignment is a powerful technique to achieve significant degrees of freedom for the interference channel. However, perfect channel state information (CSI) is assumed. Our objective is to characterize the effect of channel estimation error on interference alignment for interference channels. In particular, we wish to obtain scaling laws that govern the relationship between achievable degrees of freedom and channel estimation error. An appropriate channel estimation scheme for our problem is the maximum likelihood (ML) channel estimation procedure. An error model based on the ML scheme is used in conjunction with interference alignment.**

I. MAXIMUM LIKELIHOOD CHANNEL ESTIMATION: ERROR MODEL

Interference alignment assumes that all channel coefficients are known *a priori* to all transmitters and receivers. We consider the following channel error model. Given channel matrices $H^{[ij]}$ from transmitter j to receiver i, entries of these matrices are independent, identically distributed (i.i.d) and zero-mean circularly symmetric complex Gaussian (ZMCSCG). We employ genie-based ML estimation of $H^{[ij]}$ [1] and, in particular, use the procedure developed in [2].

Consider a vector channel model

$$Y = HX + Z \tag{1}$$

Let N_t be the number of transmit antennas and N_r number of receive antennas ($N_r \geq N_t$). Assume a code of block length N. Then X is a $N_t \times N$ matrix of transmitted signal, Y is a $N_r \times N$ matrix of received signal, H is a $N_r \times N_t$ complex random matrix with i.i.d ZMCSCG entries with unit variance, Z is a $N_r \times N$ noise matrix with ZMCSCG entries with variance N_o. The noise at the receiver is both spatially and temporally white: $E[ZZ^\dagger] = NN_oI_{N_r}$. There is the usual power constraint on the transmitted signal.

We assume that the transmitter sends a pilot matrix X_{P_L} of dimensions $N_t \times N_{P_L}$ and a data matrix X. Let the average pilot symbol energy be denoted by E_{P_L}. At the receiver we have:

$$Y = HX + Z \tag{2}$$

$$Y_{P_L} = HX_{P_L} + Z_{P_L} \tag{3}$$

We need to estimate a $N_r \times N_t$ matrix H so at least N_rN_t independent measurements are required. At every symbol instant we have N_r measurements so we require that length of pilot symbols $N_{P_L} \geq N_t$. Also we require that $X_{P_L}X_{P_L}^\dagger$ be invertible.

Let $\hat{H}_{ML}$ denote the ML estimate of H. We have [2]

$$\begin{aligned}\hat{H}_{ML} &= Y_{P_L}X_{P_L}^\dagger(X_{P_L}X_{P_L}^\dagger)^{-1} \\ &= H + \Delta H\end{aligned} \tag{4}$$

Note that H and ΔH are independent, and by employing an orthogonal pilot matrix X_{P_L} we can show that ΔH is a white noise matrix whose entries are i.i.d ZMCSCG and the variance of the entries is $N_o/(N_{P_L}E_{P_L})$ and its covariance matrix is $(N_o/(N_{P_L}E_{P_L}))I_{N_t}$.

II. 3 USER MIMO INTERFERENCE CHANNEL

Consider a 3 user ($K = 3$) MIMO interference channel with M antennas at each node. For this channel $3M/2$ degrees of freedom can be obtained with constant channel matrices with $M > 1$ antennas at each node [3]. Each user has $M/2$ degrees of freedom yielding a total of $3M/2$ degrees of freedom for the network.

To illustrate the effect of channel estimation error on interference alignment, consider a 3 user interference channel with $M = 2$ antennas. Interference alignment is performed using $\hat{H}_{ML}^{[ij]}$ from transmitter j ($j = 1,2,3$) to receiver i ($i = 1,2,3$). Noting that $\hat{H}_{ML}^{[ij]} = H^{[ij]} + \Delta H^{[ij]}$, let us consider the received signal at receiver 1 ($i = 1$):

$$\begin{aligned}Y^{[1]} = {} & H^{[11]}V^{[1]}X^{[1]} + H^{[12]}V^{[2]}X^{[2]} + H^{[13]}V^{[3]}X^{[3]} \\ & + \Delta H^{[11]}V^{[1]}X^{[1]} + \Delta H^{[12]}V^{[2]}X^{[2]} + \Delta H^{[13]}V^{[3]}X^{[3]} \\ & + Z^{[1]}\end{aligned} \tag{5}$$

where $V^{[j]}$ and $X^{[j]}$ represent the alignment and input vectors respectively corresponding to transmitter j.

Once the set of appropriate alignment vectors U^1 has been chosen, U^1 is orthogonal to both $H^{[12]}V^{[2]}$ and $H^{[13]}V^{[3]}$, and interference terms due to transmitters 2 and 3 are canceled. Thus we have:

$$\begin{aligned} y_1 &= < Y^{[1]}, U^1 > \\ &= < H^{[11]}V^{[1]} + \Delta H^{[11]}V^{[1]}, U^1 > X^{[1]} + \\ &\quad < \Delta H^{[12]}V^{[2]}, U^1 > X^{[2]} + < \Delta H^{[13]}V^{[3]}, U^1 > X^{[3]} \end{aligned} \tag{6}$$

Note that if we were to have perfect channel estimation, that is, $\Delta H^{[ij]} = 0$, we have would have full degrees of freedom. So the effect of white noise matrices is to introduce interference, and we would want the estimation error to scale as the inverse of the SNR.

References

[1] T. L. Marzetta, "Blast Training: Estimating Channel Characteristics for High Capacity Space-Time Wireless," *Proceedings 37th Annual Allerton Conference on Communication, Control, and Computing, Monticello, IL*, Sept. 22-24 1999.

[2] G. Taricco and E. Biglieri, "Space-Time Decoding With Imperfect Channel Estimation," *IEEE Trans. Wireless Commun.*, vol. 4, no. 4, pp. 1874–1888, July 2005.

[3] V. R. Cadambe and S. A. Jafar, "Interference Alignment and the Degrees of Freedom for the K User Interference Channel," *arXiv: 0707.0323, preprint*.